MATERIAL AND THERMAL ANALYSIS OF LASER SINTERTED PRODUCTS

Radovan HUDÁK[*], Martin ŠARIK[*], Róbert DADEJ[*], Jozef ŽIVČÁK[*], Daniela HARACHOVÁ[**]

[*]Faculty of Mechanical Engineering, Department of Biomedical Engineering and Measurement, Technical University of Košice,
Letná 9, 042 00 Košice, Slovakia
[**]Faculty of Mechanical Engineering, Department of Machine Design, Transport and Logistic, Technical University of Košice,
Letná 9, 042 00 Košice,   Slovakia

radovan.hudak@tuke.sk, martin.sarik@tuke.sk, robert.dadej@tuke.sk, jozef.zivcak@tuke.sk, daniela.harachova@tuke.sk

Abstract: Thermal analysis of laser processes can be used to predict thermal stresses and consequently deformation in a completed part. Analysis of temperature is also the basic for feedback of laser processing parameters in manufacturing. The quality of laser sintered parts greatly depends on proper selection of the input processing parameters, material properties and support creation. In order to relatively big heat stress in the built part during sintering process, the thermal simulation and thermal analysis, which could help better understand and solve the issue of parts deformations is very important. Main aim of presented work is to prepare input parameters for thermal simulations by the use of RadTherm software (Thermoanalytics Inc., USA), directly during the sintering process and after the process and find out the impact of the heat stress on a final shape and size of the prototype. Subsequently, an annealing process of constructed products after DMLS could be simulated and specified.

Key words: Material Analysis, Direct Metal Laser Sintering, Thermal Analysis, Deformations, Thermal Analyzing Software, Metrotomography

1. INTRODUCTION

Laser sintering or selective laser sintering (SLS) is an additive manufacturing technique that uses a high power laser to fuse small particles Fig. 1, of plastic, metal (DMLS), ceramic, or glass powders into a mass that has a desired three-dimensional shape (http://www.substech.com/dokuwiki/doku.php?id=sinteringofmeta). It is kind of thermal treatment of a loose metal powder or compact at temperature below melting point of the main constituent, for purpose of increasing its strength by bonding together of the particles. Laser selectively fuses powdered material by scanning cross-sections generated from a three dimensional (3D) digital model of the part designed by computer-aided design (CAD) on the surface of powder bed. After each cross-section is scanned, the powder bed is lowered by one layer thickness, than a new layer of material is applied on top, and the process is repeated until the part is completed (http://www.substech.com/dokuwiki/doku.php?id=sinteringofmeta).

Laser sintering is complicated because of its fast laser scan rates and material transformations in a very short timeframe. The temperature field was found to be inhomogeneous by many previous researchers (Wang et al., 2002; Kruth et al., 2003; Simchi, 2006; Kolossov et al., 2004; Zhang et al., 2010). Thermal distortion of the fabricated part is one of the main issues in selective laser melting SLM (Contuzzi et al., 2011). Meanwhile, the temperature evolution history in laser sintering has significant effects on the quality of the final parts, such as density, dimensions, mechanical properties, microstructure, etc. for metals, large thermal gradients increase residual stresses and deformation, and may even lead to crack formation in the fabricated part (Zeng et al., 2012). A case study of main characteristics of LS temperature distribution and effects of process parameters to temperature was summarized by Zeng, Pal and Stucker (Zeng et al., 2012).

The goal of this study was to analyze the intraosseal dental implants in aspect of material and surface properties and prepare the methodology of thermal analysis of product during and after manufacturing process by DMLS technology.

2. MATERIAL AND METHODS

Material analysis was realized by the use of electron microscope analysis, EDX analysis, and measurement of hardness. EDX analysis (Energy-Dispersive X-Ray) is analysis of chemical composition of surface layer of the tested part. Observation was performed by microscope JEOL JSM-7000F, with analyzer INCAx - sight from Oxford Instruments and microscope JEOL JSM-35CF, with analyzer LINK AN 10/85S. For the measurement of microhardness was used light microscope with microhardness device Hanemann, applicated load was 50 g. Microhardness was measured on samples which were polished and fine burned, due to the detection of grain boundaries. The five values on eight samples were measured on each sample, and average value was calculated. Samples were sorted form Ti1 to Ti8. Material of samples was titanium alloy intended to use in biomedical applications. Testing models were fabricated using Ti64 material from EOS Company (EOS GmbH, Germany). EOS Titanium alloy Ti64 is a pre-alloyed Ti6AIV4 alloy in a fine powder form. Parts built from EOS Ti64 fulfil the requirements of ASTM F1472 regarding maximum concentration of impurities. Physical and mechanical properties of EOS Ti64 are – density: 4430 kg/m3, thermal conductivity: $\lambda = 6.6$ W/mK, melting temperature: $T = 1670 ˚C$, tensile strength: $R_m = 1150 ± 60$ MPa. Inert atmosphere was represented by argon (Ar) gas atmosphere as environment in process chamber during the sintering process. Thermal conductivity of argon: $\lambda = 0.016$ W/mK.

Typical sintering furnace has three zones, first is preheating zone – for remove lubricant and other organic material, second is sintering zone – where the diffusion occurs and last is cooling zone – where the sintered parts cooled down. The EOSINT M 280 (EOS GmbH Germany) was used for DMLS process. The system is equipped with a solid state 200 watts laser which provides high quality radiation and stable performance. Process chamber consists of three systems, shown in Fig. 1, building system 21 dm3, dispenser system 26 dm3 and a collector system 13 dm3. Building system contains building platform with these parameters: wide (W) x high (H): 250 x 250 mm, thickness: thk = 22 mm, material – 1.1730 tools steel, surface: mechanical machined. General technical parameters of EOSINT M 280 are minimum recommended layer thickness: 30µm, value of volume in time is about: 3 mm3/s, minimum wall thickness: 0.3 – 0.4 mm and surface roughness: Ra = 0.36 – 0.48.
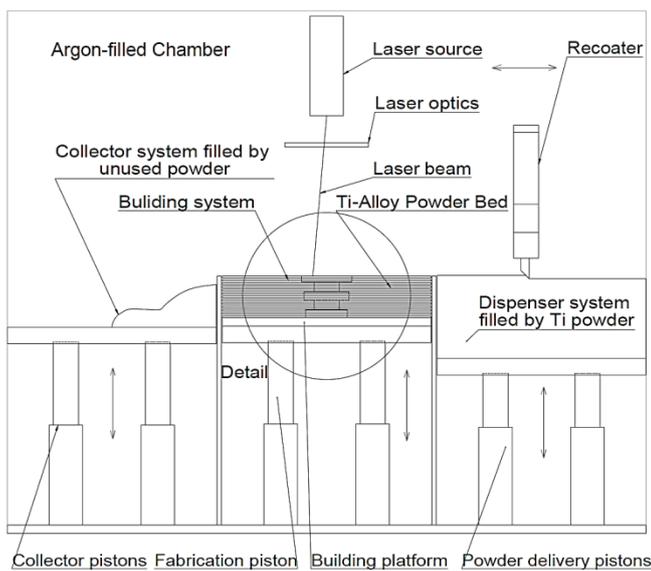
**Fig. 1.** Scheme of DMLS process on machine EOSINT M 280 detail of building platform is shown below
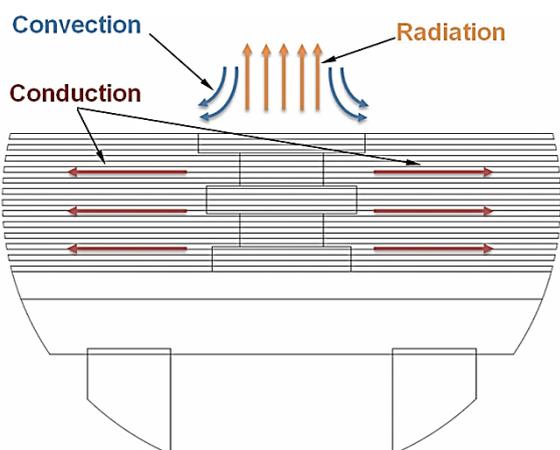
Fig. 2. Detail of building platform with three modes of heat transfer shown by different colors

Metrotomographic machine Metrotom 1500 (Carl Zeiss, Germany) was used for the purposes of visual and quantitative expressions of deformations of pre-prepared samples with these technical parameters – the maximum size of measured compo-

nents (x, y, z): 300 x 300 x 300 mm, maximum weight of parts: 50 kg, power source: 225 kV / 225 W, resolution detector: 1024 x 1024 points and safety: steel housing with lead cladding meets the standards of DIN 54113 needed for full protection operator.

The testing model created for purposes of thermal analysis was designed in 3D CAD software SolidWorks (Dassault Systèmes SolidWorks Corporation USA, CANADA). Testing model and dimension changes after DMLS process caused by heat stress are shown on Fig. 3.
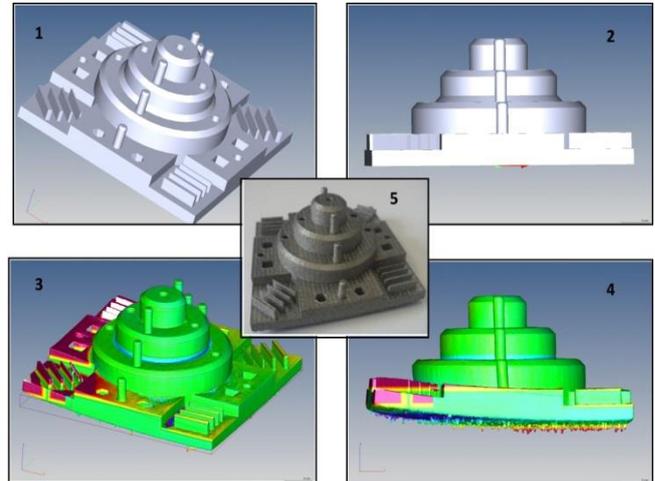
Fig. 3. Base 3D model (3.1, 3.2), base 3D model (3.3, 3.4) in comparison with built, after scanning in Metrotom 1500 (visualization of defor-mation)

The heat stresses and thermal changes are affecting dimensions and shapes of fabricated parts, what requires an adequate heat treatment (Kulesza et al., 2012; Praslicka et al., 2013). As each part is different and many parameters can be changed, it is important to predict and simulate heat processes (stresses) before the DMLS process of 3D printing. For modeling and simulation of heat conduction and fabricated parts finite element deformation analysis during and post – DMLS processes several software applications can be used.

SINDA/FLUINT (Network Analysis Inc., USA) is tool for design of thermal distribution and fluid flow analysis in complex systems. Another application is FloEFD (FlowSim Pty Ltd., Australia), which is analytic tool with strong connection on main MCAD systems.

The RadTherm (Thermoanalytics Inc., USA) is thermal analyzing software based on finite element method analysis, which was implemented in to the simulation algorithms. RadTherm solves the energy balance equation simultaneously for convection, conduction, and radiation. All temperature and heat load data are input as constants or as functions of time at user discretion. RadTherm utilizes the time-averaging Crank-Nicholson implicit finite difference scheme to discretize the governing equations (http://www.thermoanalytics.com/products/radtherm).

After importing the 3D geometry in appropriate thermal analysis software was very important to set the boundary conditions.

Classical Fourier heat transfer equations are the most common for describing the temperature distribution. Based on the Fourier equation, various models have been developed by combing latent heat, material thermal property nonlinearity, laser heat source distribution and interaction between a laser beam and powder bed (http://www.thermoanalytics.com/products/radtherm, Jiangui et al., 2008; Jiang et al., 2002l Baojun and Fazhong, 2002).

Heat transfer is that section of engineering science that studies the energy transport between material bodies due to a temperature difference (Lienhard IV and Lienhard V, 2012; Lewis et al., 2004; Vozda et al., 2012). During the sintering process and cooling phase of sintered parts are thermal conduction and thermal convection very important modes for data collection and evaluation of heat effects. So there is need to define main equations for next work.

Tab. 1. Input and output parameters for thermal simulation in RadTherm

Input Parameters	Output Parameters
Density – ρ [kg/m³]	Temperature of each element – T_E [°C]
Specific heat – c_p [J/kgK]	
Thickness of part – th_P [mm]	Temperature range of each element – $T_{Emax} - T_{Emin}$ [°C]
Thickness of powder layer – th_L [mm]	
Thermal conduction – λ [W/mK]	Maximum reached temperature – T_{max} [°C]
Convective heat transfer coefficient – h_C [W/m²K]	
Temperature of medium (Ar) – T_{Ar} [°C]	Minimum reached temperature – T_{min} [°C]
Volume of medium (Ar) – V_{Ar} [m³]	
Temperature of preheating – T_P [°C]	Plot of temperature vs. time – T/t [°C/s]
Time of preheating – t_P [s]	
Sintering temperature – T_S [°C]	The course of temperatures in time – [s]
Time of sintering – t_S [s]	
Cooling temperature - T_C [°C]	Velocity of heating in time – T_{VH}/t [°C/s]
Time of cooling – t_C [s]	
Heat capacity – C [J/m³K]	Velocity of cooling in time – T_{VC}/t [°C/s]
Number of layers – n_L	

Thermal Convection consists of two forms, either forced (artificial) and helpful or natural and free form. Next formula presents the convection heat transfer through a surface area at specific temperatures:

$$q = h_c A dT \tag{1}$$

where: q – is transferred heat per unit of time [W], A – is surface area of heat transfer [m2], h_c – is convective heat transfer coefficient [W/m2K] or [W/m2°C], dT – is difference of temperature among surface and volume of fluid [K] or [°C].

Thermal Conduction is the transfer of heat between substances that are directly in contact to each other. The conduction mode of heat transport occurs either because of an exchange of energy from one molecule to another, without the actual motion of the molecules, or because of the motion of the free electrons if they are present. Equation to calculate the necessary heat to increase the temperature of body only if between temperatures will not be phase change.

$$Q = cm(t - t_0) \tag{2}$$

where: Q – is heat [J], c – is specific heat capacity [Jkg-1K-1], m – is weight [kg], $(t - t_0)$ – reduction of a new temperature from the initial temperature [K].

In (3) is calculation of heat conduction between two ends of metal stick where temperatures are T1 and T2.

$$\Delta Q = \frac{\lambda S(T_2 - T_1)}{L} \Delta t \tag{3}$$

where: λ – is specific heat conductivity [Wm−1K−1], t – is time [s], S – is cross-section of stick [mm2] and L – is length of stick [mm].

In publication (Baojun and Fazhong, 2002) was steady state heat conduction in one dimension described by the equation for a plane wall, shown in equation (4):

$$kA\frac{d^2T}{dx^2} = 0 \tag{4}$$

where k – is the thermal conductivity and a is the cross-sectional area perpendicular to the direction of heat flow. The problem is complete with following description of the boundary conditions: At $x = 0, T = T_1$, and at $x = L, T = T_2$,
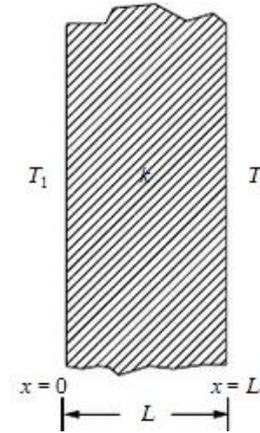

Fig. 4. Heat conduction through a homogenous wall

The exact solution to Eq. (4) is:

$$kAT = C_1 x + C_2 \tag{5}$$

On applying the appropriate boundary conditions to Eq. (5) we obtain:

$$C_2 = kAT_1 \tag{6}$$

$$C_1 = -\frac{kA(T_1 - T_2)}{L} \tag{7}$$

Therefore, substituting constants C1 and C2 into Eq. (5) results in:

$$T = -\frac{(T_1 - T_2)}{L} x + T_1 \tag{8}$$

The above equation indicates that the temperature distribution within the wall is linear. The heat flow, Q can be written as:

$$Q = -kA\frac{dT}{dx} = -\frac{kA}{L}(T_2 - T_1) \tag{9}$$

Above presented equations are the bases for a next complex heat and heat stress analysis of DMLS processes and post-processes and post-fabrication using simulation software's.

3. RESULTS

Material analysis was in this case realized with reason of; obtain the values of material composition, visualization of the surfaces, evaluation of microstructure, fracture surfaces and microhardness of samples. The surfaces of the samples were observed and documented with light microscopy and also scanning electron microscopy. Results from observing are shown in Fig. 5.
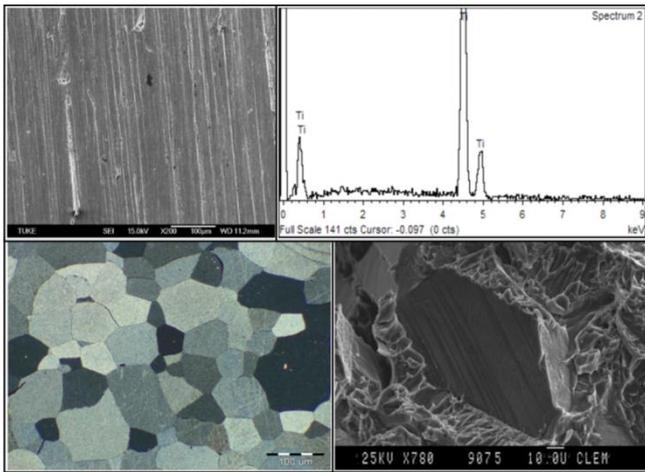
Fig. 5. Observation of the surface and EDX material analysis of Ti1 (up left and right), Microstructure of Ti1 (down left) and Evaluation of surfaces fractures (down right)

Tab. 2. Result from microhardness (MH) measurement [HV0.05]

Sample	Average value of microhardness	Standard deviation of microhardness
Ti1	242.5	15.36229
Ti2	256.2	16.16663
Ti3	248.9	29.56078
Ti4	254.9	18.72538
Ti5	283.2	19.00947
Ti6	307	8.94427
Ti7	301.2	9.92773
Ti8	314.4	37.51053

On the prepared samples was performed observation and EDX analysis of the surface, observation of microstructure and fracture surfaces of the samples and measurement of microhardness. EDX analysis of the surface samples shows that samples of Ti1, Ti2, Ti3 and Ti4 consist of pure titanium. Any trace levels of contaminants is not possible, respectively is problematic to determine by EDX analysis.

EDX analysis of polished sections of samples Ti5, Ti6, Ti7 and Ti8 confirmed, that they contains from pure titanium. By EDX analysis of dull sections was found that in addition to titanium is in analysis the relatively high content of aluminum (Al), oxygen (O$_2$) and carbon (C). It can be assumed that at least part of the carbon and oxygen comes from pollution of samples, despite the fact that all samples were cleaned before observing in methanol and in ultrasonic cleaner. Despite the mixed results, which concerns the content of individual elements is necessary this EDX analysis perceive rather only as a qualitative and semi-qualitative than quantitative. Thus, the measured differences in contents of individual element, it is impossible to talk about the different surfaces of samples Ti5, Ti6, Ti7 and Ti8. From the findings show, that all samples are made of pure titanium, the surface of four of them (samples Ti5, Ti6, Ti7 and Ti8) is partially corundum blast.

The observation of the microstructure of the samples shows, that the structure of the sample Ti1, Ti2, Ti3 and Ti4 is quite heterogeneous and consists of polyhedral grains of size 20 to 150 microns. The structure of the samples Ti5, Ti6, Ti7 and Ti8 is relatively homogeneous and consists of polyhedral grains in size from 5 to 15 microns. In case of problematic preparation of

matallographic sections from titanium, not all documented microstructures were in sufficient quality. Grain size (GS) was not statistically recorded but only roughly compared.

On the samples was measured microhardness HV 0, 05. While for the samples Ti1, Ti2, Ti3 and Ti4 were average measured values in the range of 240 – 260 HV units, the samples Ti5, Ti6, Ti7 and Ti 8 were average measured values in the range of 295 – 315 HV units. The maximum standard deviation of microhardness measurement was 37.51053 HV. The results of microhardness measurements may have been more decisively influenced by different grain size, and thus area of impress considering the size of grain.

In Fig. 6. is possible to observe the first results of thermal simulation preformed with use of RadTherm software. It shows the simulation of stress relieving process after sintering process.
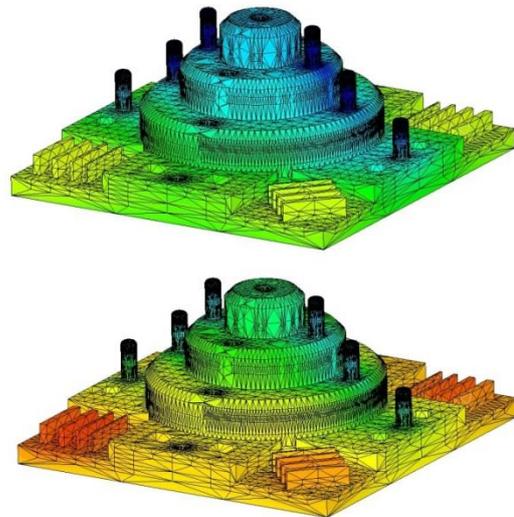
Fig. 6. The test sample during the stress relieving process simulation, the upper and lower sample with a gradual transition of heat from the edges to the center (core)

4. CONCLUSIONS

Presented paper shows results of two studies, analysis of the intraosseal dental implants from material and surface properties point of view and preparation of the methodology for thermal analysis of product during and after manufacturing process using DMLS technology.

Regarding to use of titanium alloys for biomedical applications, was prepared the material analysis, where were described and measured values of grain size and microhardness.

EDX analysis was performed for analyzing of comercially available implants, which are made from pure titanium (cp Ti) (Sidun and Dąbrowski, 2009).

In process of preparation is next study where will be analyzed outputs from DMLS technology (EOSINT M280, EOS Germany), but in the first case it will be necessary to perform analysis and simulation of heat processes and subsequently analyisis of dimensional circuits for detection of differences in term of residual heat stresses.

Attention was also taken to preparation of input parameters for heat and heat stress analysis. These input parameters must be prepared before the each research. It is only first phase

of planned studies. It defines the main issues and describes the technical aspects of DMLS and technology process of manufacturing the prototypes. In next research should be included fact that during the DMLS process all layers are not sintered homogeneously but in predefined laser beam pattern. To get exact parameters for heat analysis will be important to place of thermocamera in to the process chamber to get to full process thermography record. For next study the multi-layer building process will be considered where conduction of previous and next layer and influence of Ti64 powder bed will be included in calculations.

REFERENCES

1. **Baojun ZHAO, Fazhong Shi,** (2002), Modeling of Selective Laser Sintering for PC Powder, *Journal of Beijing University of Aeronautics and Astronautics*, Vol.28, No. 6, 660-663.
2. **Contuzzi,N.,Campanelli,S.L., et al.** (2011), 3D Finite element analysis in the selective laser melting process, *Int. J. Simul Model*, Vol. 10, No. 3, 113-121.
3. **Jiang Wei, Dalgarno K.W., et al.** (2002), *Finite Element Analysis of Residual Stresses and Deformations in Direct Metal SLS Process*, [cited on 2012-10-18], available at: http://edge.rit.edu/content/ P10551/public/SFF/SFF%202002%20Proceedings/2002%20SFF%2 0Papers/38-Jiang.pdf
4. **Jiangui Li, Yusheng Shi, et al.** (2008), Numerical Simulation of Transient Temperature Field in Selective Laser Melting, *China Mechanical Engineering*, Vol 19, No. 20, 2492-2495.
5. **Kolossov S., Boillat E., et al.** (2004), 3D FE simulation for temperature evolution in the selective laser sintering process, *International Journal of Machine Tools and Manufacture*, Vol. 44, No. 2-3, 117-123.
6. **Kruth J.P., Wang X., et al.** (2003), Lasers and materials in selective laser sintering, *Assembly Automation*, Vol. 23, No. 4, 357 – 371.
7. **Kulesza E., Dabrowski J.R., Sidun J., Neyman A., Mizera J.** (2012) Fretting wear of materials – Methodological aspects of research, *Acta Mechanica et Automatica*, Vol. 6, No. 3, 58-61.
8. **Lewis R. W., et al.** (2004), *Fundamentals of the Finite Element Method for Heat and Fluid Flow*, Wiley, 356.
9. **Lienhard IV, H. J., Lienhard V, H. J.,** (2012), *A Heat Transfer Textbook, Fourth Edition*, Phlogiston PressCambridge, Massachusetts, U.S.A.
10. **Praslička D., Blažek J., Šmelko M., Hudák J., Čverha A., Mikita I., Varga R., Zhukov A.,** (2013), Possibilities of measuring stress and health monitoring in materials using contact-less sensor based on magnetic microwires, *IEEE Transactions on Magnetics*, 49 (1), art. no. 6392407, 128-131.
11. **RadTherm® Heat Transfer Analysis Software,** [cited on 2012-10-18], available at: http://www.thermoanalytics.com/products/radtherm
12. **Sidun J., Dabrowski J.R.,** (2009), Bone ingrowth processes on porous metallic implants, Diffusion and Defect Data Pt.B: *Solid State Phenomena*, Volume 147-149, 776-781.
13. **Simchi A.** (2006), Direct laser sintering of metal powders: Mechanism, kinetics and microstructural features, *Materials Science and Engineering*: A 428, Vol. 1, No. 2, 148-158.
14. **SINTERING OF METALS.** [cited on 2012-10-18], available at: http://www.substech.com/dokuwiki/doku.php?id=sinteringofmetals
15. **Vozda M., Sekora M., Penhaker M.,** (2012), Precise Temperature Stabilizing System of Liquids for the Purpose Biomedical Alications, *Journal Electronics and Electrical Engineering*, Vol.18, No. 10, 29 – 32.
16. **Wang X. C., Laoui T., et al.** (2002), Direct Selective Laser Sintering of Hard Metal Powders: Experimental Study and Simulation, *Int J Adv. Manuf. Technol.*, Vol.19, 351–357.
17. **Zeng, K. Pal, D. Stucker, B.** (2012), *A review of thermal analysis methods in Laser Sintering and Selective Laser Melting*, [cited on 2012-10-18], available at: http://utwired.engr.utexas.edu/lff/sympo sium/proceedingsArchive/pubs/Manuscripts/2012/2012-60-Zeng.pdf
18. **Zhang D. Q., Cai Q. Z., et al.** (2010), Select laser melting of W–Ni–Fe powders: simulation and experimental study, *The International Journal of Advanced Manufacturing Technology*, Vol. 51, No. 5-8, 649-658.